J|A|C|S COMMUNICATIONS

Published on Web 03/10/2009

Dumbbell-like Au−Fe_3O_4 Nanoparticles for Target-Specific Platin Delivery

Chenjie Xu, Baodui Wang,† and Shouheng Sun*

Department of Chemistry, Brown University, Providence, Rhode Island 02912

Received February 1, 2009; E-mail: ssun@brown.edu

Pt-based platin complexes, such as cisplatin, carboplatin, and oxaliplatin (Figure 1A), are well-known generations of anticancer therapeutic agents.[1] One common feature of these square-planar Pt complexes is that they all contain Pt−N/Pt−Cl or Pt−N/Pt−O coordination bonds with two Pt−N bonds in the cis position. The Pt−Cl or Pt−O bonds in these complexes are chemically much weaker than the Pt−N bonds and subject to facile hydrolysis under low Cl^- and/or low pH conditions, giving charged *cis*-$[Pt(NH_3)_2(H_2O)_2]^{2+}$ complexes that are highly reactive for DNA binding through the N7 atom of either an adenine or guanine base. This binding destacks the double-helix structure and interrupts the cell's genetics/transcription machinery and repair mechanism, leading to cell death.[2] However, these powerful platin therapeutic agents have no capability to identify tumor cells from healthy ones. As a result, they tend to be taken up by any rapidly grown cells, tumorous and healthy ones alike, causing the well-known toxic side effects.[3]

Here we report that dumbbell-like Au−Fe_3O_4 nanoparticles (NPs) can act as target-specific nanocarriers to deliver platin into Her2-positive breast cancer cells with strong therapeutic effects. Recent research progress has revealed that antigens are often overexpressed on the surfaces of the rapidly growing tumor cells. These overexpressed antigens provide obvious targets for specific binding, as each type of antigen can be selectively captured by a typical monoclonal antibody.[4] Therefore, when linked with a monoclonal antibody, these carriers may achieve target-specific delivery through strong antibody−antigen interactions and receptor-mediated endocytosis. The dumbbell-like Au−Fe_3O_4 NPs offer an ideal platform for this delivery purpose. As shown in Figure 1B, their core structure contains magnetic Fe_3O_4 NPs and optically active Au NPs. Compared with the conventional single-component iron oxide NPs used for biomedical applications,[5] the dumbbell-like Au−Fe_3O_4 NPs have the following distinct advantages: (1) the presence of Fe_3O_4 and Au surfaces facilitates the stepwise attachment of an antibody and a platin complex, and (2) the structure can serve as both a magnetic and optical probe for tracking the platin complex in cells and biological systems.

To produce Au−Fe_3O_4 NPs for target-specific platin delivery, we first synthesized the dumbbell-like Au−Fe_3O_4 NPs using a published method;[6] a series of dumbbell-like NPs are shown in Figure S1 in the Supporting Information. As an example, the oleate/oleylamine-coated 8 nm/18 nm Au−Fe_3O_4 NPs (Figure S1C) were functionalized by replacing the oleate/oleylamine with dopamine- and thiol-based surfactants (Figure 1B).[7] In this structure, the platin complex was anchored on the Au side by reacting Au−S−$CH_2CH_2N(CH_2COOH)_2$ with cisplatin, and the Her2-specific monoclonal antibody Herceptin chosen as a targeting agent was linked to Fe_3O_4 through PEG_{3000}−CONH−Herceptin.[7] The Au−Fe_3O_4−Herceptin linkage was confirmed using matrix-assisted laser desorption ionization (MALDI) mass spectrometry (Figure S2), while the platin−Au conjugation was characterized by inductively coupled plasma atomic emission spectroscopy (ICP−AES) and energy dispersive spectroscopy (EDS). The elemental analyses revealed that the conjugate contains an atomic S/Pt ratio of ∼1/1 (Figure S3). This indicates that two carboxylic groups replace the two Cl ligands in cisplatin to form the platin complex, as shown in Figure 1B. According to the Pt/Au weight percentage (∼17.8%), ∼2812 platin units are bound to each Au NP.[7] We also characterized the size-dependent platin loading on the Au−Fe_3O_4 NPs. Among the 3/18, 6/18, 8/18, and 8 nm/25 nm Au−Fe_3O_4 NPs tested, the larger Au NPs were capable of incorporating more platin complexes, while the size of the Fe_3O_4 NP had little effect on the platin concentration (Table S1). This further proves that platin binds to the Au side and not to the Fe_3O_4 side, as shown in Figure 1B. The final conjugate can be dispersed in PBS. The 8 nm/18 nm Au−Fe_3O_4 NPs had a 32 nm hydrodynamic diameter, as measured by dynamic light scattering (Figure S4).

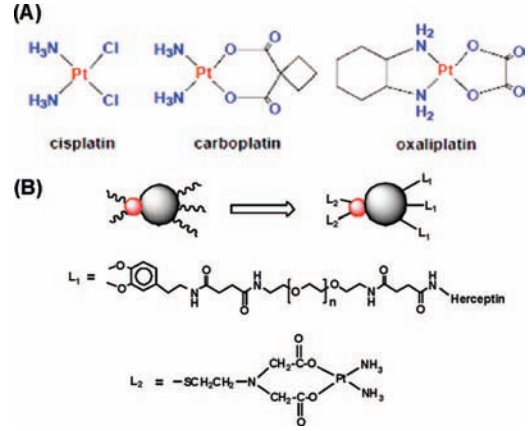

Figure 1. (A) Structures of the common therapeutic platin complexes. (B) Schematic illustration of the dumbbell-like Au−Fe_3O_4 NPs coupled with Herceptin and a platin complex for target-specific platin delivery.

The specificity of the platin−Au−Fe_3O_4−Herceptin NPs was examined through their preferred targeting of Sk-Br3 cells that are Her2-positive breast cancer cells [Her2-negative breast cancer cells (MCF-7) were used as a control].[8] Before incubation with the platin−Au−Fe_3O_4−Herceptin NPs, Sk-Br3 and MCF-7 cells were preblocked with 1% BSA. The cells were then incubated with the NPs in PBS for 1 h and fixed with 4% paraformaldehyde. The cells were later imaged using a Leica TCS SP2 AOBS spectral confocal microscope at 594 nm, the region where the Au NPs show a strong reflection.[9] Figure 2 shows reflection images of Sk-Br3 cells (Figure 2A) and MCF-7 cells (Figure 2B). The brighter image (∼1.5 times brighter as measured through Image J) shown in Figure 2A indicates that more platin−Au−Fe_3O_4−Herceptin NPs target the Sk-Br3 cells. We can conclude that under the same incubation concentration, Herceptin helps the preferred targeting of Sk-Br3 cells as opposed

† Current address: College of Chemistry and Chemical Engineering and State Key Laboratory of Applied Organic Chemistry, Lanzhou University, Lanzhou 730000, P.R. China.

10.1021/ja900790v CCC: $40.75

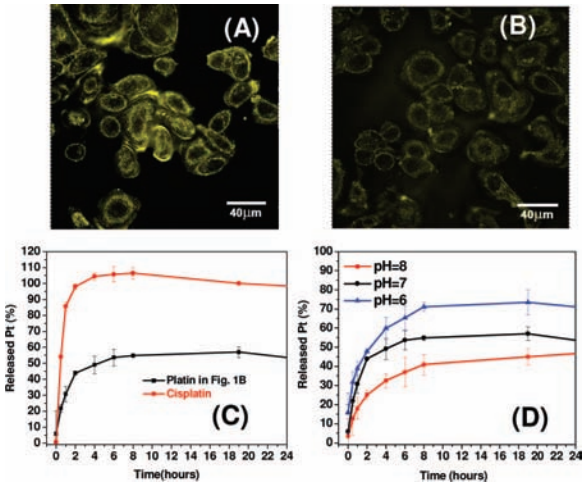

Figure 2. Reflection images of (A) Sk-Br3 and (B) MCF-7 cells after incubation with the same concentration of platin−Au−Fe_3O_4−Herceptin NPs. (C) Cisplatin and platin release curves at 37 °C (pH 7). (D) pH-dependent Pt release from platin−Au−Fe_3O_4−Herceptin at 37 °C.

to MCF-7 cells. Transmission electron microscopy image analysis of the Sk-Br3 cells reveals the presence of NPs in the endosome/lysosome, which indicates that the NPs were taken up through the endocytosis process (Figure S5).

Platin release from the NP conjugate (100 μg of Pt in 2 mL of PBS) was analyzed in a dialysis bag (MWCO = 1000) that was put into a 30 mL reservoir of PBS at 37 °C. Cisplatin with the same Pt concentration was used as a control. The membrane of the dialysis bag kept the bound platin and NPs inside the bag while the released platin or free cisplatin could diffuse into the buffer reservoir, whose Pt concentration was measured by ICP−AES. The platin-release data are given in Figure 2C. It can be seen that 80% of the free cisplatin diffused through the dialysis bag in 1 h, while for the NP conjugate, this release was reduced to only ~25% in the same incubation time. Furthermore, the Pt release was pH-dependent (Figure 2D). At pH 6, 70% of the platin was released from the platin−Au−Fe_3O_4−Herceptin NPs after 10 h, while at pH 8, the amount of platin release was reduced to 40%. Clearly, lower pH conditions accelerate the release of platin from the conjugate shown in Figure 1B. As endosome/lysosome has a pH of ~5, we can conclude that platin release will be accelerated once the conjugate is taken inside the cells through endocytosis.

The therapeutic effect of the platin−Au−Fe_3O_4−Herceptin NPs was studied by measuring the cell viability and p53 expression in Sk-Br3 cells. The control experiments showed that Au−Fe_3O_4 NPs without platin did not inhibit cell growth at any of the Fe concentrations tested (Figure S6A). Once coupled with platin, however, the platin−Au−Fe_3O_4−Herceptin NPs had half-maximal inhibitory concentration (IC_{50}) toward Sk-Br3 cells of 1.76 μg of Pt/mL (Figure 3), which is lower than that needed for cisplatin (3.5 μg/mL). It should be noted that the platin−Au−Fe_3O_4 NPs without Herceptin were also toxic, but their toxicity was less than that of cisplatin because of their nonspecificity and the slow platin hydrolysis in the conjugate. The fact that the highest toxicity toward Sk-Br3 cells was observed for the platin−Au−Fe_3O_4−Herceptin NPs is clearly attributed to the specific targeting and enhanced uptake of these NPs by Sk-Br3 cells. In contrast, platin−Au−Fe_3O_4−Herceptin NPs did not show obvious improvement in their toxicity toward MCF-7 cells (Figure S6B).

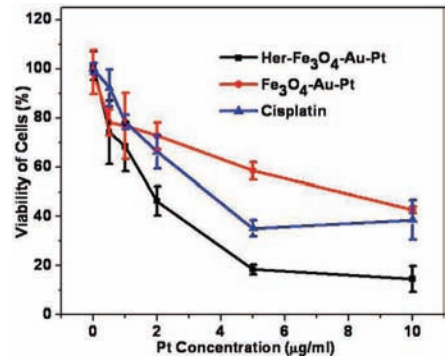

Figure 3. Viability of Sk-Br3 cells after incubation with platin−Au−Fe_3O_4 NPs, platin−Au−Fe_3O_4−Herceptin NPs, and free cisplatin.

The increase in Pt concentration within Sk-Br3 cells can also be monitored by the accumulation of p53, a tumor-suppressor protein.[10] It was easily seen in a control experiment that more p53 was present with a higher concentration of cisplatin added in the cell culture medium with β-actin as the loading control (Figure S6C).[7] We tested the p53 protein expression in Sk-Br3 cells after treatment with different NPs and cisplatin. The cells treated with platin−Au−Fe_3O_4−Herceptin NPs had the highest p53 expression (Figure S6D). This is consistent with what we observed in the cell-toxicity data in Figure 3, indicating that Herceptin indeed induces more uptake of platin into the Sk-Br cells, which has a highly toxic effect on these cells.

In summary, we have demonstrated that dumbbell-like Au−Fe_3O_4 NPs can serve as a multifunctional platform for target-specific platin delivery. The release of the therapeutic platin under low-pH conditions renders the NP conjugate more toxic to the targeted tumor cells than to free cisplatin. The methodology developed here can be generalized, and the dumbbell-like Au−Fe_3O_4 NPs should therefore have great potential as nanocarrriers for highly sensitive diagnostic and highly efficient therapeutic applications.

Acknowledgment. The work was supported by NIH/NCI 1R21-CA12859. Herceptin was provided by Prof. Xiaoyuan Chen of Stanford University.

Supporting Information Available: Experimental procedures, Figures S1−S6, and Table S1. This material is available free of charge via the Internet at http://pubs.acs.org.

References

(1) Jamieson, E. R.; Lippard, S. J. *Chem. Rev.* **1999**, *99*, 2467–2498.
(2) (a) Kelland, L. *Nat. Rev. Cancer* **2007**, *7*, 573–584. (b) Wang, D.; Lippard, S. J. *Nat. Rev. Drug Discovery* **2005**, *4*, 307–320.
(3) (a) Siddik, Z. H. *Oncogene* **2003**, *22*, 7265–7279. (b) Gately, D. P.; Howell, S. B. *Br. J. Cancer* **1993**, *67*, 1171–1176.
(4) Adams, G. P.; Weiner, L. M. *Nat. Biotechnol.* **2005**, *23*, 1147–1157.
(5) (a) Sun, C.; Lee, J. S. H.; Zhang, M. Q. *Adv. Drug Delivery Rev.* **2008**, *60*, 1252–1265. (b) Jun, Y. W.; Lee, J. H.; Cheon, J. W. *Angew. Chem., Int. Ed.* **2008**, *47*, 5122–5135.
(6) Yu, H.; Chen, M.; Rice, P. M.; Wang, S. X.; White, R. L.; Sun, S. H. *Nano Lett.* **2005**, *5*, 379–382.
(7) See the Supporting Information.
(8) Daly, J. M.; Jannot, C. B.; Beerli, R. R.; GrausPorta, D.; Maurer, F. G.; Hynes, N. E. *Cancer Res.* **1997**, *57*, 3804–3811.
(9) Xu, C. J.; Xie, J.; Ho, D.; Wang, C.; Kohler, N.; Walsh, E.; Morgan, J.; Chin, Y. E.; Sun, S. H. *Angew. Chem., Int. Ed.* **2008**, *47*, 173–176.
(10) Yazlovitskaya, E. M.; DeHaan, R. D.; Persons, D. L. *Biochem. Biophys. Res. Commun.* **2001**, *283*, 732–737.

JA900790V